ESTIMATION OF FRACTION OF ABSORBED PHOTOSYNTHETICALLY ACTIVE RADIATION FROM MULTIPLE SATELLITE DATA

Xin Tao, Shunlin Liang, Fellow, IEEE, Tao He

Department of Geographical Sciences, University of Maryland, College Park, MD 20742, USA

ABSTRACT

Fraction of Absorbed Photosynthetically Active Radiation (FPAR) is a critical input parameter in many climate and ecological models. An accuracy of ±0.1 in FPAR is considered acceptable in the applications. However, most of current FPAR products, such as Moderate-Resolution Imaging Spectroradiometer (MODIS) and Multi-angle Imaging SpectroRadiometer (MISR), do not fulfill the accuracy requirement yet. The objective is to develop a new radiative transfer model for FPAR estimation, with broadened surface reflectance database from the time series of twelve years' reflectance data. The model proposed here could successfully identify growing season and the time series curve of estimated FPAR was smooth over years. The R^2 between estimated FPAR and in situ measurements was improved compared to existing FPAR products.

Index Terms— FPAR, radiative transfer, retrieval

1. INTRODUCTION

Radiation fluxes at the Earth's surface play important roles in many ecological, climatological, and hydrological systems. The Fraction of Absorbed Photosynthetically Active Radiation (FAPAR, or FPAR) is the fraction of incoming solar radiation in the spectral range from 400 nm to 700 nm that is absorbed by plants. It is a critical input parameter in the biogeophysical and biogeochemical processes described by many climate and ecological models (e.g. Community Land Model, Community Earth System Model, crop growth models). The accuracy in calculating FAPAR, often from remote sensing measurements, directly influences estimates of net primary productivity (NPP) and carbon cycle [1].

As early as the FIFE field experiment, the remotely sensed FPAR were declared to be accurate within a range of 10% in the experiment [2]. Fang et al. [3] indicates that MODIS C5 products have a high correspondence with field measurements and the R^2 reached 0.6 for woody biomes. FPAR in Collection 5 are supposed to be accurate as new stochastic RT model could capture the 3D effects of foliage clumping and species mixtures of natural ecosystems. Some other studies on ecosystems, however, reported that MODIS overestimate FPAR of most ecosystems compared with field data [4]. The 3D RT algorithm of MODIS yields high FPAR values versus the tram value of approximately zero for an ecosystem after fire [5].

This study focuses on improving estimations of FPAR from multiple satellite data. A radiative transfer algorithm is proposed to retrieve from multiple data sources including MOD09 reflectance and MISR L2 HDRF data. The retrieved FPAR values are further validated with field measurements.

2. METHODOLOGY

In moderate resolution images, vegetation pixels are almost continuously distributed across large regions in the imagery. Radiative transfer model for continuous canopy is chosen for FPAR retrieval [6][7]. The formulas proposed here include reflective anisotropic characteristics caused by sun-target-sensor geometry and neglect reflective anisotropic characteristics caused by soil background and leaf canopy. It calculates canopy absorption from canopy transmittance and reflectance, and considers single and multiple scattering in the canopy. The basic formula is like [8]:

$$\mathrm{FPAR}=\int_{400nm}^{700nm}\int_{0}^{\pi/2}[\left(1-T_0-2\rho_{\mathrm{v},\lambda}\right)+\left(1-T_{\mathrm{v}}(\theta)-2\rho_{\mathrm{v},\lambda}\right)\frac{T_0\rho_{\mathrm{g},\lambda}}{1-\rho_{\mathrm{g},\lambda}\rho_{\mathrm{v},\lambda}}]d\theta d\lambda$$

$$T_0=\exp(-\lambda_0\frac{G_{\mathrm{s}}}{\mu_{\mathrm{s}}}LAI)$$

$$\rho_{\mathrm{v},\lambda}=\rho_{\mathrm{c},\lambda}\left[1-\exp\left(-\lambda_0\frac{G_{\mathrm{v}}}{\mu_{\mathrm{v}}(\theta)}\Gamma(\phi)LAI\right)\right]+$$

$$\beta\rho_{\mathrm{c},\lambda}\left[\exp\left(-\lambda_0\frac{G_{\mathrm{v}}}{\mu_{\mathrm{v}}(\theta)}\Gamma(\phi)LAI\right)-\exp\left(-\lambda_0\frac{G_{\mathrm{v}}}{\mu_{\mathrm{v}}(\theta)}LAI\right)\right]$$

where T_0 is canopy transmittance along the light penetrating path, $\rho_{\mathrm{g},\lambda}$ and $\rho_{\mathrm{v},\lambda}$ are the hemispherical albedos of the soil background and the vegetation respectively. λ_0 is the Nilson parameter accounting for the vegetation clumping effect, μ_{s} and $\mu_{\mathrm{v}}(\theta)$ are cosine values of the solar and view zenith angle (θ), β is the ratio of scattering light; G_{s} and G_{v} are the mean projection of a unit foliage area along the solar and viewing direction respectively:

$$G_{\mathrm{s,v}}=\frac{1}{2\pi}\int_{2\pi}g_{\mathrm{L}}(\Omega_{\mathrm{L}})\left|\Omega_{\mathrm{L}}\cdot\Omega_{\mathrm{s,v}}\right|d\Omega_{\mathrm{L}}$$

where $1/2\pi \cdot g_L(\Omega_L)$ is the probability density of the distribution of the leaf normals with respect to the upper hemisphere, i.e. leaf angle distribution [9]. The empirical function $\Gamma(\phi)$ describes the hot-spot phenomenon, $\Gamma(\phi) = \exp\left(\frac{-\phi}{180-\phi}\right)$ where the symbol ϕ accounts for the sun-target-sensor position and depends on the angle between the solar and viewing direction and the leaf angle distribution of canopy.

MODIS utilizes a maximum of only 29 patterns of effective ground reflectance at the spectral bands in the LUT. Different from this, the input data of the soil background and vegetation canopy reflectance will be derived from a database built upon the time series of twelve years' reflectance data. The database will be a broad extension of the input for the existing algorithm. Fig. 1 shows an example of the soil reflectance database and vegetation reflectance at peak season for MODIS tile H10V04.

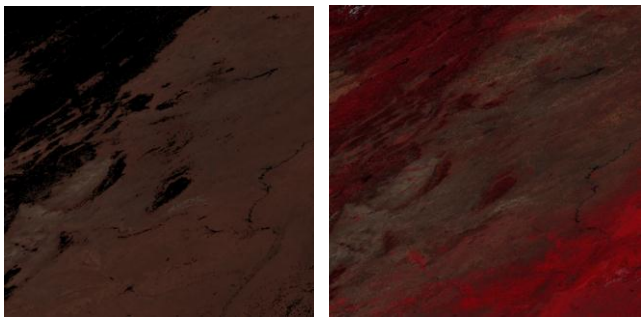

Fig. 1 Soil and vegetation reflectance database for MODIS tile H10V04 built upon twelve years' reflectance data (NIR-R-G false color composition).

3. VALIDATION SITES

Fig. 2 shows the distribution of VAlidation of Land European Remote sensing Instruments Sites (VALERI) and AmeriFlux sites for validation. In total, there are 37 sites including 17 forests, 10 crops, 9 grasslands and 1 shrubland. The details for the two AmeriFlux sites are listed in table 1.

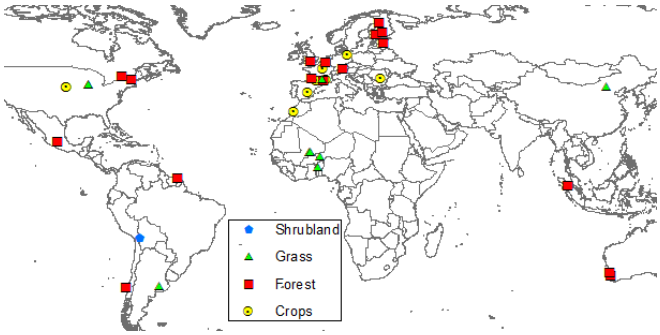

Fig. 2 The distribution of the VALERI and AmeriFlux sites

Table 1 List of AmeriFlux sites for validation

Site	Latitude (°)	Longitude (°)	Land Cover
Mead Irrigated	41.1651	-96.4766	Croplands
Mead Rainfed	41.1797	-96.4396	Croplands
Bartlett	44.0646	-71.2881	DBF*

*DBF: Deciduous Broadleaf Forests

4. RESULTS

MODIS LAI and FPAR products and the estimated LAI and FPAR from MOD09 reflectance were compared to field measurements of VALERI, as shown in Fig. 3. It seems that MODIS has underestimated LAI at these sites. MODIS FPAR are better estimated than LAI regarding bias, r-square and RMSE. The estimated LAI from MOD09 reflectance data have been overestimated compared to field-measured LAI, but the correlation with field data is better compared to MODIS products. Both MODIS FPAR product and estimated FPAR from MOD09 are little biased, but estimated FPAR have better correlation with field data than MODIS FPAR product do.

The time series of MODIS and MISR products and FPAR *in situ* measurements were plotted in Fig. 4 at the three AmeriFlux sites since 2006 for 2 or 3 years. Due to fewer valid observations, MISR products are depicted as dots. MODIS products are in lines. The MISR FPAR is higher than those from MODIS, especially in the middle of the vegetation growth season. The FPAR at Mead Irrigated (MI) and Rainfed (MR) reaches zero before early April and after middle November, which must be due to the harvest of the crop there. Satellite product values of FPAR around the two sites approach but are not exactly zero at the beginning and end of the year, which may be caused by the contribution from inhomogeneous land cover in addition to cropland near the sites or the limited soil reflectance database used by the algorithm. The errors for FPAR products are listed in Table 2.

Fig. 5 shows the time series of FPAR *in situ* measurements and the estimated FPAR from MODIS and MISR at the three AmeriFlux sites. For all of the three sites, the r-square has increased using the proposed model (Table 3). The improvement is most apparent at the Bartlett experimental forest site (Bl), where the r-square of MODIS FPAR is improved from 0.641 to 0.745, and that of MISR from 0.657 to 0.806. Similarly, the r-square of estimated FPAR from MODIS is improved from 0.667 to 0.773, and that from MISR from 0.761 to 0.84 at the Mead Irrigated site. The improvement at Mead Rainfed site is minor, and statistics show that the r-square of estimated FPAR from MODIS is increased from 0.626 and 0.632, and that from MISR, from 0.638 to 0.784.

As observed in Fig. 4, most products are not that good compared with field measurements at the two cropland sites due to the unsuccessful detection of the vegetation growth season. However, the model proposed here utilized both

simple ratio (SR) and more accurate soil reflectance data and successfully identified growing season. Moreover, the time series curve of the estimated FPAR is smooth over the year. However, there still exists some underestimation in the latter half of the year, or at the end of the growing season specifically, which is caused by the senescence and yellow turning of the leaves and thus the FPAR from remote sensing (green FPAR) is different from measurements (total FPAR) here.

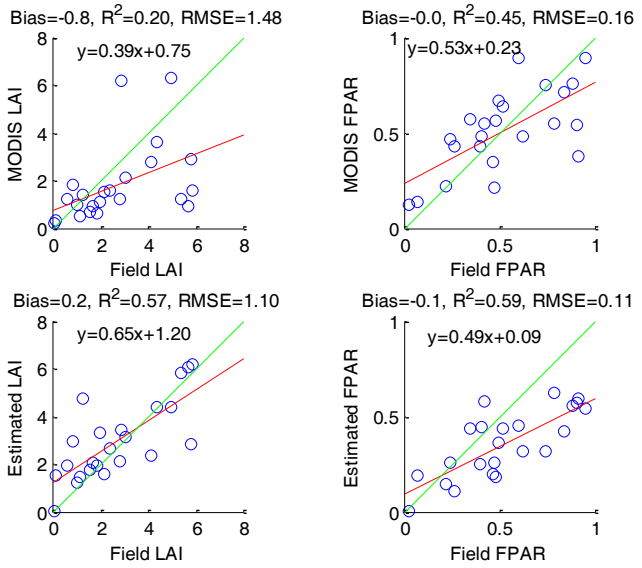

Fig. 3 MODIS LAI and FPAR compared to field measurements of VALERI.

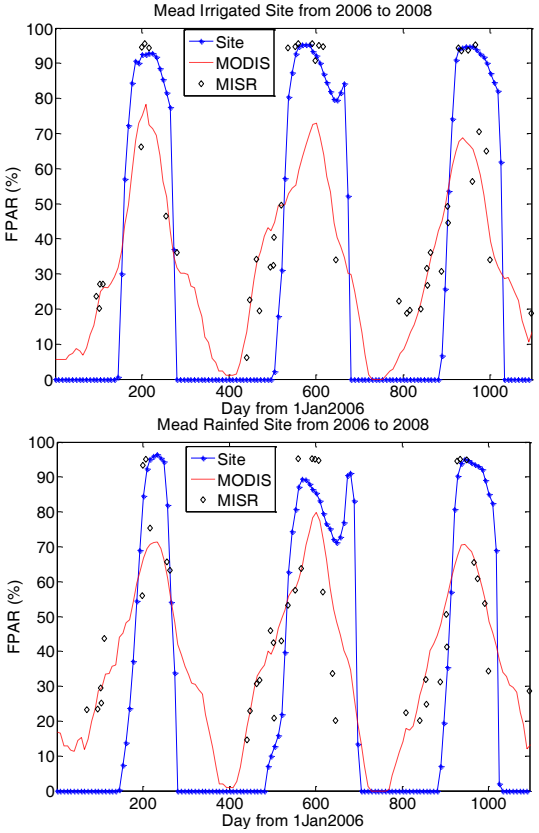

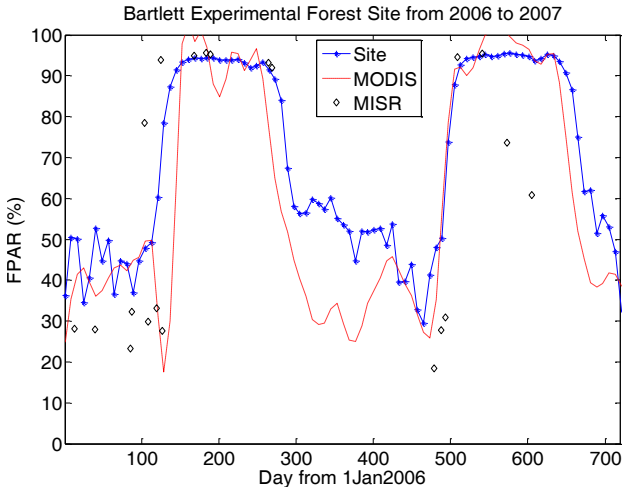

Fig. 4 The time series of *in situ* measurements and FPAR products at three AmeriFlux sites.

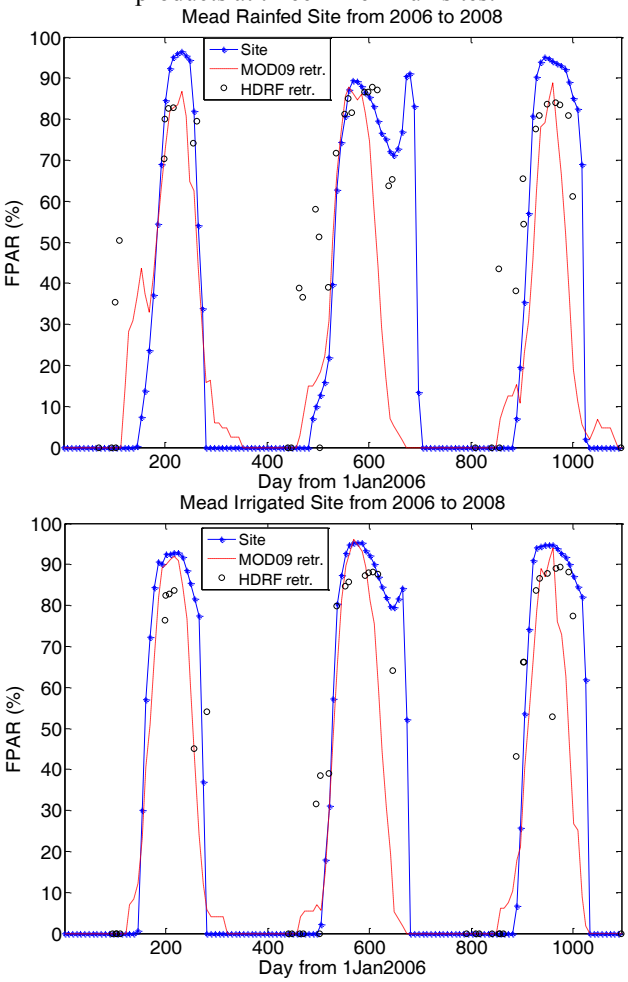

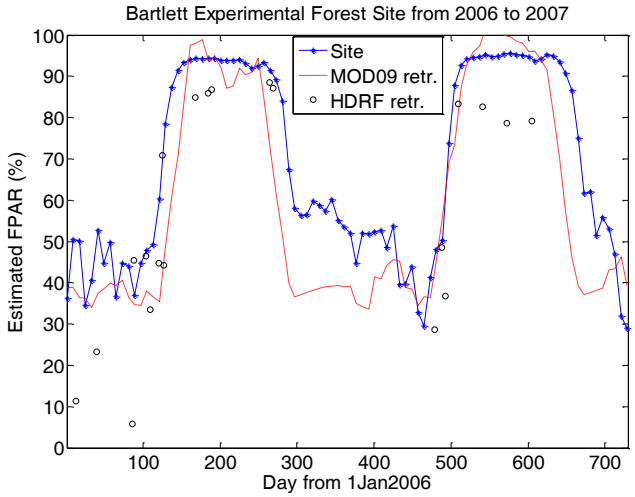

Fig. 5 The time series of i*n situ* measurements and estimated FPAR from MODIS and MISR at the three AmeriFlux sites.

Table 2 The errors of FPAR products compared to field measurements

Site	Product	Mean err	Std err	Bias	R-square
MI	MODIS	0.212	0.145	0.009	0.667
	MISR	0.193	0.142	0.072	0.761
MR	MODIS	0.214	0.143	0.07	0.626
	MISR	0.219	0.125	0.043	0.638
Bl	MODIS	0.129	0.146	-0.083	0.641
	MISR	0.175	0.131	-0.108	0.657

Table 3 The errors of estimated FPAR compared to field measurements

Site	Estimated	Mean err	Std err	Bias	R-square
MI	MODIS	0.103	0.189	-0.083	0.773
	MISR	0.101	0.148	0.005	0.84
MR	MODIS	0.133	0.207	-0.069	0.632
	MISR	0.132	0.149	0.058	0.784
Bl	MODIS	0.119	0.103	-0.089	0.745
	MISR	0.141	0.115	-0.132	0.806

5. CONCLUSIONS

The intercomparison among FPAR products show that MISR products are generally 10% higher than MODIS products. This agrees with the results from other researchers (e.g. [10]). Estimated FPAR from HDRF of MISR and reflectance of MOD09 using the presented model agree better with each other than the products, which can be due to the same algorithm applied. FPAR products did not detect well zero FPAR values outside the growing season at cropland sites. The model proposed here utilized both SR and more accurate soil reflectance data and successfully identified growing season. Moreover, the time series curve of estimated FPAR is smooth over year. There still exists some underestimation in the latter half of the year, or at the end of the growing season specifically, which is caused by the senescence and yellow turning of the leaves and thus the difference between the FPAR from remote sensing, which is green FPAR and that from measurements, which is total FPAR here. Future work will examine this issue by using field measurements of green FPAR.

6. REFERENCES

[1] M. Zhao and S.W. Running, "Drought-Induced Reduction in Global Terrestrial Net Primary Production from 2000 through 2009," *Science*, vol. 329, no. 5994, pp. 940-943, 2010.

[2] F. G. Hall, K.F. Huemmrich, S.J. Goetz, P.J. Sellers, and J.E. Nickeson, "SATELLITE REMOTE-SENSING OF SURFACE-ENERGY BALANCE - SUCCESS, FAILURES, AND UNRESOLVED ISSUES IN FIFE," *Journal of Geophysical Research-Atmospheres,* vol. 97, no. D17, pp. 19061-19089, 1992.

[3] H. Fang, S. Wei, and S. Liang, "Validation of MODIS and CYCLOPES LAI products using global field measurement data," *Remote Sensing of Environment,* vol. 119, pp. 43-54, 2012.

[4] R. Fensholt, I. Sandholt, M. Schultz, "Evaluation of MODIS LAI, fAPAR and the relation between fAPAR and NDVI in a semi-arid environment using in situ measurements," *Remote Sensing of Environment,* vol. 91, pp. 490-507, 2004.

[5] Y.F. Cheng, J.A. Gamon, D.A. Fuentes, Z.Y. Mao, D.A. Sims, H.L. Qiu, H. Claudio, A. Huete, and A.F. Rahman, "A multi-scale analysis of dynamic optical signals in a Southern California chaparral ecosystem: A comparison of field, AVIRIS and MODIS data," *Remote Sensing of Environment,* vol. 103, pp. 369-378, 2006.

[6] Y. Knyazikhin, J.V. Martonchik, R.B. Myneni, D.J. Diner, and S.W. Running, "Synergistic algorithm for estimating vegetation canopy leaf area index and fraction of absorbed photosynthetically active radiation from MODIS and MISR data," *Journal of Geophysical Research-Atmospheres*, vol. 103, no. D24, pp. 32257-32275, 1998.

[7] S. Liang, A.H. Strahler, X. Jin, and Q. Zhu, "Comparisons of radiative transfer models of vegetation canopies and laboratory measurements," *Remote Sensing of Environment*, vol. 61, no. 1, pp. 129-138, 1997.

[8] X. Tao, B. Yan, K. Wang, D. Wu, W. Fan, X. Xu, and S. Liang, "Scale transformation of leaf area index product retrieved from multi-resolution remotely sensed data: analysis and case studies," *International Journal of Remote Sensing*, vol. 30, no. 20, pp. 5383-5395, 2009.

[9] S. Liang, *Quantitative Remote Sensing of Land Surfaces*. John Wiley & Sons, Inc., New York, 2004.

[10] N. Gobron, B. Pinty, M.M. Verstraete, J. Widlowski, and D.J. Diner, "Uniqueness of multiangular measurements - Part II: Joint retrieval of vegetation structure and photosynthetic activity from MISR," *IEEE Trans. Geosci. Remote Sens.*, vol. 40, no. 7, pp. 1574-1592, 2002.